Clinical Neurophysiology 125 (2014) 277–286

Contents lists available at ScienceDirect

Clinical Neurophysiology

journal homepage: www.elsevier.com/locate/clinph

The alteration of spontaneous low frequency oscillations caused by acute electromagnetic fields exposure

Bin Lv [a,b,1], Zhiye Chen [c,1], Tongning Wu [a], Qing Shao [a], Duo Yan [b], Lin Ma [c,*], Ke Lu [b,*], Yi Xie [a,*]

[a] China Academy of Telecommunication Research of Ministry of Industry and Information Technology, Beijing, China
[b] University of Chinese Academy of Sciences, Beijing, China
[c] Department of Radiology, PLA General Hospital, Beijing, China

ARTICLE INFO

Article history:
Accepted 20 July 2013
Available online 4 September 2013

Keywords:
Radiofrequency electromagnetic fields
Long Term Evolution
Resting state fMRI
Amplitude of low frequency fluctuation

HIGHLIGHTS

- The resting state fMRI was applied to investigate the Long Term Evolution (LTE) radiofrequency electromagnetic field (RF-EMF) exposure influence on spontaneous brain activity.
- A controlled LTE RF-EMF exposure environment was designed, and the amplitude of low frequency fluctuation (ALFF) and fractional ALFF (fALFF) approaches were selected to analyze the resting state fMRI signals.
- We found the spontaneous low frequency oscillations in brain were altered by the acute LTE RF-EMF exposure.

ABSTRACT

Objective: The motivation of this study is to evaluate the possible alteration of regional resting state brain activity induced by the acute radiofrequency electromagnetic field (RF-EMF) exposure (30 min) of Long Term Evolution (LTE) signal.
Methods: We designed a controllable near-field LTE RF-EMF exposure environment. Eighteen subjects participated in a double-blind, crossover, randomized and counterbalanced experiment including two sessions (real and sham exposure). The radiation source was close to the right ear. Then the resting state fMRI signals of human brain were collected before and after the exposure in both sessions. We measured the amplitude of low frequency fluctuation (ALFF) and fractional ALFF (fALFF) to characterize the spontaneous brain activity.
Results: We found the decreased ALFF value around in left superior temporal gyrus, left middle temporal gyrus, right superior temporal gyrus, right medial frontal gyrus and right paracentral lobule after the real exposure. And the decreased fALFF value was also detected in right medial frontal gyrus and right paracentral lobule.
Conclusions: The study provided the evidences that 30 min LTE RF-EMF exposure modulated the spontaneous low frequency fluctuations in some brain regions.
Significance: With resting state fMRI, we found the alteration of spontaneous low frequency fluctuations induced by the acute LTE RF-EMF exposure.

Abbreviations: LTE, Long Term Evolution; RF-EMF, radiofrequency electromagnetic fields; ALFF, amplitude of low frequency fluctuation; fALFF, fractional amplitude of low frequency fluctuation; STG_L, left superior temporal gyrus; MTG_L, left middle temporal gyrus; STG_R, right superior temporal gyrus; MFG_R, right medial frontal gyrus; PCL_R, right paracentral lobule.

* Corresponding authors. Address: Department of Radiology, PLA General Hospital, No. 28, Fuxing Road, Beijing 100853, China. Tel.: +86 10 66939592 (L. Ma). University of Chinese Academy of Sciences, No. 19A, Yuquan Road, Beijing 100049, China. Tel./fax: +86 10 88256595 (K. Lu). China Academy of Telecommunication Research of Ministry of Industry and Information Technology, No. 52, Huayuanbei Road, Beijing 100191, China. Tel.: +86 10 62301646 (Y. Xie).
E-mail addresses: cjr.malin@vip.163.com (L. Ma), luk@ucas.ac.cn (K. Lu), xieyi@catr.cn (Y. Xie).
[1] These authors contributed equally to this work.

1388-2457/$36.00
http://dx.doi.org/10.1016/j.clinph.2013.07.018

1. Introduction

With the increasing use of mobile phone, more and more attention has been paid to the possible health effects of radiofrequency electromagnetic fields (RF-EMF) Barnes et al., 2008; Patrick et al., 2008. Among the various endpoints in human biological effects of RF-EMF, human laboratory study is a direct approach which is designed to evaluate the effects of RF-EMF exposure in a controlled laboratory environment (Barnes et al., 2008). Particularly, most studies are mainly focused on the possible RF-EMF effects in term of brain activity and function. During the past few years, many approaches have been used to investigate the brain electrophysiological and neurometabolic effects of mobile phone related RF-EMF (Valentini et al., 2007; Kwon and Hamalainen, 2011). Electroencephalography (EEG) studies provided the electrophysiological evidences about the effect of RF-EMF at different frequency bands during resting (Croft et al., 2002; Curcio et al., 2005), sleeping (Huber et al., 2002) and event-related or evoked potentials (Curcio et al., 2005; Kleinlogel et al., 2008). Neuroimage studies with Positron emission tomography (PET) measured the changes of regional cerebral blood flow (rCBF) Huber et al., 2002; Haarala et al., 2003; Aalto et al., 2006 or the brain glucose metabolism (Volkow et al., 2011) to assess the cumulative effects of cell phone exposure on brain. Although the results of these studies are not always consistent, the findings have increased our understanding of RF-EMF influence on human brain.

Functional magnetic resonance imaging (fMRI), which is based on the principle of blood oxygenation level dependent (BOLD), is another widely used neuroimage technique to measure the brain hemodynamic changes (Logothetis and Wandell, 2004). The BOLD signals will change in response to the underlying neural events or neuronal processes when a stimulus or task is performed (Logothetis and Wandell, 2004). Furthermore, even during the resting state, there are still spontaneous low frequency fluctuations of BOLD signals which are related to the intrinsic neuronal activities and have very important physiological significances (Fox and Raichle, 2007). Many resting-state fMRI studies have reported that the spontaneous neural activities are highly synchronous in some district brain areas, such as between the bilateral motor cortical areas (Biswal et al., 1995), within the language network (Hampson et al., 2002) and within the default mode network (Greicius et al., 2003). In order to detect the regional property of spontaneous fluctuation in BOLD signal, a local measure called amplitude of low frequency fluctuations (ALFF) is proposed which calculates the averaged square root of power spectrum within a specific low frequency range (typically 0.01–0.1 Hz) (Zang et al., 2007). Then a normalized index of ALFF called fractional ALFF (fALFF), which can reduce the sensitivity to physiological noise, is obtained by taking the ratio of power spectrum of a specific low frequency range to that of the entire frequency range (e.g. 0–0.25 Hz) Zou et al., 2008. Previous study has investigated their test-retest reliability (Zuo et al., 2010). And both measures have been utilized to investigate the pattern of spontaneous brain activity in normal subjects (Zuo et al., 2010) and their alternation in patients with attention deficit hyperactivity disorder (Zang et al., 2007), Alzheimer's disease (He et al., 2007) and schizophrenia (Hoptman et al., 2010). Using the fMRI technique, a recent study investigated the brain BOLD response changes induced by an exposure of Global System for Mobile Communication (GSM) signal when participants were trained to perform a somatosensory Go-NoGo task (Curcio et al., 2012). The result showed that they did not find any change in BOLD response and cognitive performance after exposed by GSM signal for 45 min. To the best of our knowledge, this is the only one task-based fMRI study to evaluate the acute effects of RF-EMF exposure, and there is no report about resting state fMRI on this area. Whether the short-term RF-EMF exposure modulates the spontaneous resting-state BOLD fluctuations in human brain still needs to be confirmed.

Most previous RF-EMF exposure studies are focused on GSM (Croft et al., 2002; Huber et al., 2002; Haarala et al., 2003; Curcio et al., 2005; Aalto et al., 2006; Kleinlogel et al., 2008; Volkow et al., 2011; Curcio et al., 2012) and Universal Mobile Telecommunication System (UMTS) Kleinlogel et al., 2008. GSM network operates in 900 and 1800 MHz frequency bands, while UMTS network operates mostly in 2100 MHz band. As one of the fourth generation of mobile phone telecommunication standards, Long Term Evolution (LTE) telecommunication networks either by frequency-division duplex (FDD) or by time-division duplex (TDD) have already been deployed or will soon be put into commercial operation in many regions (Parkvall et al., 2011). Its frequency bands range from 800 up to 3500 MHz. As a relative new type of RF-EMF, it is necessary to investigate the effect of LTE-related exposure. In addition, most previous studies used the commercial mobile phone as the exposure source (Croft et al., 2002; Huber et al., 2002; Aalto et al., 2006; Volkow et al., 2011; Curcio et al., 2012). This experimental design might bring about the heating effect or the sound noise (Huber et al., 2002; Haarala et al., 2003). And it is hardly to maintain the same emission power in repetitive experiment. Therefore, it is better to setup the controlled electromagnetic field environment for exposure experiment.

In this study, we designed a double-blind, crossover, randomized and counterbalanced study to explore the possibility of altered regional resting state brain activity induced by the near-field LTE RF-EMF exposure. Each subject participated in real and sham exposure separated by 1 day. The LTE signal was emitted by a dipole antenna, and the electromagnetic field was controllable in order to maintain the same exposure condition for each subject as much as possible. Resting state BOLD fMRI signals of human brain were collected before and after the 30 min RF-EMF exposures. Then we utilized ALFF (Zang et al., 2007) and fALFF (Zou et al., 2008) methods to investigate the possible exposure-induced changes in the amplitude of spontaneous fluctuations. We want to evaluate whether the subjects in this experiment show the different low frequency oscillations in some brain areas after the acute RF-EMF exposure of LTE signal.

2. Methods

2.1. Subjects

In this study, eighteen right-handed healthy subjects were recruited through the advertisement on campus Bulletin Board System (BBS). There are twelve males and six females, and the age range is from 19 to 35 years (mean: 24.9 ± 3.9 years). The inclusion criteria included: (a) no history of brain injury; (b) no history of neurological disease or any other obvious illness that may influence the brain function; (c) be compatible with an MRI scan. Subjects were instructed to abstain from alcohol and nicotine, and to maintain their regular cycle of sleep-wake the day before the experiment. They are all regular mobile phone users (less than 1 h per day), and no one used the mobile phone for more than 10 min in the whole day prior to the experiment. Written informed consent was obtained from all subjects after the experimental procedure had been fully explained. This study was approved by the ethics committee of the local institutional review board.

2.2. Experimental design

The experiment had two sessions (real and sham exposure) for each subject. During each session, the experimental procedure was designed to include three conditions in order: structural MRI and

resting-state fMRI scan, RF-EMF exposure (real or sham), and resting-state fMRI scan again. The RF-EMF exposure lasted for 30 min and therefore one session lasted about 1 h. The two sessions were separated by 1 day. The whole design was a double-blind, crossover, randomized and counterbalanced paradigm. Subjects did not know the sequence of real and sham exposure, while experiment and data analysis were finished by different people. The exposure experiment and MRI scan were performed at PLA General Hospital (Beijing, China).

2.3. Exposure setup

The LTE exposure setup was designed to radiate each subject with the identical power regardless of the power reflection due to the existence of the human. We used the standard dipole (SPEAG) as exposure source to simulate a controlled electromagnetic field environment. Fig. 1 illustrated the experimental setting. A CMW 500 (R&S) and an RF amplifier (AR) were used to generate the LTE signals at 2.573 GHz band. Dipole antenna was placed on the right side with a distance of 1 cm to the ear. The spacing distance was restricted by a white foam, and the length of the dipole was perpendicular to the head length. During the exposure, subjects were instructed to select a comfortable posture on the chair with touching the foam. They would keep quiet while being not involved in any task and hold on the condition as much as possible. The exposure experiment was carried out in an anechoic chamber.

Since the presence of the human body cause non-negligible power reflection for the nearby dipole (Standard 1528. IEEE recommended practice for determining the peak spatial-average specific absorption rate (SAR) in the human head from wireless communications devices: measurement techniques. NJ, 1528), the net power delivered to the dipole is reduced. Furthermore, the anatomical difference also induces the variation in the actual delivered power (TN, 2012). It is crucial to determine the subject-specific delivered power during the exposure experiments. Therefore, we applied the similar protocol dedicating to system check for specific absorption rate (SAR) measurement per subject in Standard 1528. IEEE recommended practice for determining the peak spatial-average specific absorption rate (SAR) in the human head from wireless communications devices: measurement techniques. NJ (1528) (Fig. 1). The reflected power could be monitored by PM2, which was compensated by adjusting the signal generator to a desired output. The net power delivered to the dipole was set to 24 dBm.

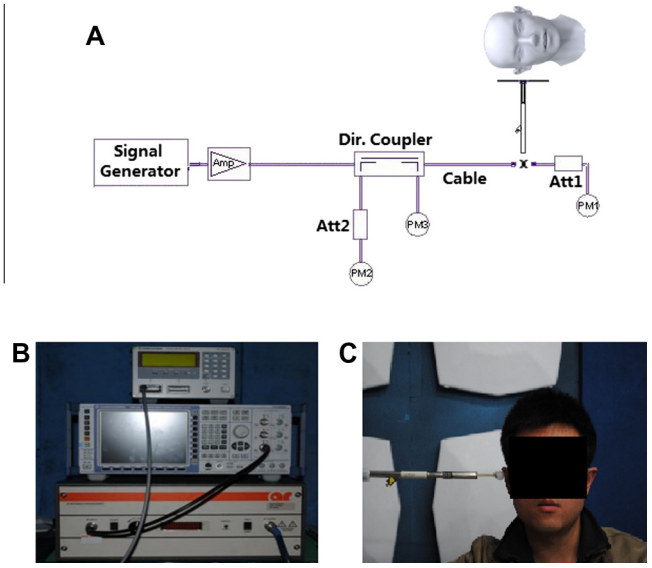

Fig. 1. Experimental setup for LTE RF-EMF exposure. (A) Flow diagram. Amp = amplifier; Dir. Coupler = directional coupler; Att = attenuator; PM = power meter. (B) Signal generator including CMW 500 (R&S) and RF amplifier (AR). (C) Dipole antenna. During experiment, subjects sit on the chair and put his/her right ear close to the dipole with the space as 1 cm restricted by the white foam.

2.4. MRI scan

All the MR data were acquired on a 3.0 T MR system (SIGNA EXCITE, GE Healthcare) with a conventional eight-channel phased array surface coil. The magnetic gradient field is 40 mT/m and the slew rate is 150 mT/m/s. During each session, subject has two MRI scans, one is performed before the RF-EMF exposure (pre-exposure scan) and the other is immediately after the exposure (post-exposure scan). Since the effect of RF-EMF on biological tissues is known to decay rapidly over time, we tried our best to shorten the time interval (about 40–50 s) between the end of the RF-EMF exposure and the actual post-exposure resting-state fMRI scan, and keep it be approximate constant as much as possible across subjects. The pre-exposure scan consisted of the high resolution T1-weighted images and the resting-state fMRI images, while post-exposure scan only included the resting-state fMRI images. The T1-weighted images were acquired by using three-dimensional fast spoiled gradient echo (3D FSPGR) sequence with parameters: repetition time (TR) = 6.8 ms, echo time (TE) = 2.9 ms, number of sagittal slices = 188, slice thickness = 1 mm, slice gap = 0 mm, field of view (FOV) = 22 × 22 cm, flip angle (FA) = 15°, matrix size = 256 × 256, in-plane resolution = 1.0 × 1.0 mm, and number of excitation (NEX) = 1. For the resting-state fMRI, the images were collected by using an echo-planar imaging (EPI) sequence with the following parameters: TR = 2 s, TE = 30 ms, slice thickness = 3 mm, slice gap = 0.8 mm, FOV = 22 × 22 cm, FA = 90°, matrix size = 64 × 64, in-plane resolution = 3.4 × 3.4 mm, NEX = 1, and 32 transverse slices to cover the whole brain volume. The pre-/post-exposure resting-state fMRI scans have the same parameters, and each scan lasted for 6 min to collect 180 image volumes. Two recent studies have investigated the impact of scan duration (Van Dijk et al., 2010; Zuo et al., 2013). Their results demonstrated that 5 min of acquisition time is enough to obtain reliable results (Van Dijk et al., 2010; Zuo et al., 2013). Therefore, our imaging scan duration is enough for current fMRI data analysis. During the scan, subjects were instructed to relax and awake with their eyes closed, and not to think of anything in particular as much as possible. At the end of each scan, subjects were asked to make sure whether they had fallen asleep, and none of them reported they had.

2.5. SAR measurement

There are two purposes for the structural images in this experiment: one is to generate the parameters of spatial normalization for functional images which will be described in the next part, and the other is to establish the head anatomical model for RF-EMF dosimetric studies (Kainz et al., 2005). Using the head anatomical model, we can measure the SAR power distribution to check the safety of LTE RF-EMF exposure condition. The process is similar to our previous preliminary work (TN, 2012).

First, the head structural images were segmented interactively to identify 24 tissues (TN, 2012) with software iSeg (Zurich Med Tech AG). Then we performed the Finite-Difference Time-Domain (FDTD) simulation Taflove and Hagness, 2005 to estimate the SAR power distribution induced in different head tissues. Protocols of numerical evaluation were defined as: FDTD spatial lattice was $1 \times 1 \times 1$ mm^3; dielectric parameters were obtained from the website (http://www.fcc.gov/oet/rfsafety/dielectric.html and http://niremf.ifac.cnr.it/tissprop/); time update step was 1.8 picoseconds; 8-layer perfectly matched layer (PML) Taflove and Hagness, 2005 has been used as absorption boundary condition, and there were

30 grids between the PML boundary and the models. The FDTD calculation was finished by using software SEMCAD X14.8 (SPEAG) and SEMF Y, 2011.

During the simulation, the half wavelength dipole antenna was also modeled. The *S* parameters were numerically simulated and compared with the measured results to ensure the consistency.

2.6. fMRI image preprocessing

The fMRI image preprocessing was carried out using Statistical Parametric Mapping software (SPM8, www.fil.ion.ucl.ac.uk/spm/) and DPARSF software (Yan and Zang, 2010). Briefly, the first ten functional volumes were discarded for the signal equilibrium and the subjects' adaptation to the scanning environment. The remaining 170 volumes were corrected for the intra-volume difference in acquisition time and the inter-volume difference in head motion. The mean functional image for each individual was generated from the corrected functional volumes. Then the corresponding T1-weighted structural image was co-registered to the mean functional image with a rigid body linear transformation. The transformed structural image was segmented into gray matter, white matter, cerebrospinal fluid with a unified segmentation algorithm (Ashburner and Friston, 2005) and generated the normalization parameters. Next, the corrected functional images were spatially normalized to the Montreal Neurological Institute (MNI) space by using the transformation parameters obtained from the unified segmentation and re-sampled into $3 \times 3 \times 3$ mm^3 resolution. After spatial normalization, the resulting functional images were further smoothed by convolution with an isotropic Gaussian kernel (full width at half maximum = 4 mm), and then removed the linear trend.

2.7. ALFF and fALFF calculation

After the image preprocessing, ALFF and fALFF were calculated from the processed functional volumes. These two measures reflect different aspects of spontaneous fluctuations in brain: ALFF indicates the absolute strength of spontaneous fluctuations within a specific frequency range, whereas fALFF represents the relative contribution of specific spontaneous fluctuations to the whole detectable frequency range (Zuo et al., 2010). To obtain them, the processed fMRI time series of each voxel was transformed to the frequency domain with a fast Fourier transform and the square root of the power spectrum was calculated at each frequency. ALFF was obtained by averaging the square root across a predefined frequency range (Zang et al., 2007). And fALFF was calculated as the ratio of ALFF in the predefined frequency range to the ALFF over the entire detectable frequency range (Zou et al., 2008). During the image preprocessing, we did not apply any temporal band-pass filter to the functional images, therefore, the detectable frequency range is from 0 to 0.25 Hz ($1/2*1/TR = 1/2*1/2 = 0.25$, where TR is the repetition time of resting-state fMRI scan). We selected the 0.01–0.1 Hz as the predefined frequency range to calculate the ALFF and fALFF values, since fMRI signals in this frequency range were mainly related to physiological meanings while the noise of very low-frequency drift and high-frequency respiratory and heart rhythms were eliminated (Biswal et al., 1995; Zuo et al., 2010). In order to reduce the global effects of variability across subjects, the ALFF/fALFF on each voxel was standardized by dividing the global mean ALFF/fALFF value (Zang et al., 2007; Zuo et al., 2010).

2.8. Statistical analysis

All statistical analysis was performed in a voxel-by-voxel manner. To determine the intrinsic whole brain patterns of spontaneous fluctuations, we first performed the within-condition analysis by applying the random-effect one-sample *t* tests on the individual ALFF/fALFF maps within each condition. Then we performed the between-condition analysis in order to detect the possible changes of spontaneous fluctuations caused by RF-EMF exposure. The random-effects paired *t* tests were applied on the ALFF/fALFF maps between pre- and post-exposure in each session (real or sham exposure). All statistical results were corrected for multiple comparisons at a significant level of $P < 0.05$ with Monte Carlo simulation method (Ledberg et al., 1998). This step was achieved by using AlphaSim program (http://afni.nih.gov/afni/docpdf/AlphaSim.pdf) with a combined threshold of $P < 0.01$ and a minimum cluster size of 513 mm^3.

In addition, we also performed the functional connectivity analysis among the different brain regions. The regions of interest (ROIs) were identified based on the results of between-condition analysis. And the mean time series of signals in each ROI were extracted from the processed fMRI signals (after linear detrend and filtered with 0.01–0.1 Hz). The correlation coefficients between ROIs were calculated and analyzed to evaluate their changes among different conditions by using one-sample *t* tests. Significant threshold was set at $P < 0.05$.

3. Results

3.1. SAR power distribution in head

During the simulation, the dipole had 1 cm distance to the right ear of head model which was the same as in the measurement. The incident power to the antenna was scaled to the measured net delivered power. Fig. 2 illustrated the results of estimated SAR power distribution in two subjects. The maximum voxel based SAR for 1 g tissue is 2.18 W/kg in Subject A and 2.36 W/kg in Subject B. Therefore, the spatial peak SAR averaging over 10 g tissue was 0.9 and 1.07 W/kg, which were less than the safety limits in ICNIRP guidelines (ICNIRP (International Commission on Non-Ionizing Radiation Protection), 1998).

3.2. Within-condition pattern of spontaneous fluctuations

Fig. 3 showed the pattern of spontaneous fluctuations detected by one-sample *t* test. Only the result of real exposure was presented since there were similar results for real and sham exposure. The top two rows illustrated the results of ALFF maps for pre- and post-exposure, while the button two rows were the results of fALFF maps. The *t* value maps were corrected using the AlphaSim procedure at $P < 0.05$. From these figures, we observed some brain regions showing the significant higher standardized ALFF/fALFF values than the globe mean ALFF/fALFF value. The regions included posterior cingulate cortex/precuneus, medial prefrontal cortex, inferior parietal lobule and occipital areas. The distributions of spontaneous fluctuations were shown as the similar pattern between the conditions of pre- and post-exposure, based on not only ALFF analysis but also fALFF analysis. Comparing the results between ALFF and fALFF maps, the significant higher ALFF values were observed in the region surrounding the bilateral lateral fissure, while much more pronounced regions were found on the frontal and occipital areas from the fALFF maps.

3.3. Between-condition difference of spontaneous fluctuations induced by exposure

The between-condition differences between pre- and post-exposure were examined based on ALFF and fALFF maps by using paired *t* tests. We did not find any between-condition difference in sham exposure. For the real exposure, we detected the

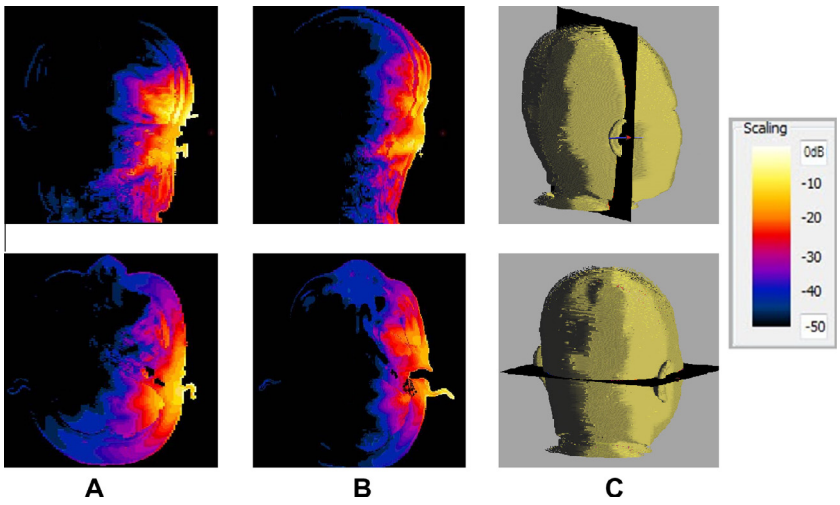

Fig. 2. Slice views for estimated SAR power distribution in two subjects (A and B). The top row is coronal view, and the button row is axial view. (C) The slice positions. SAR maps are colored according to the bar on the right, and 0 dB equals 2.36 W/kg for a specific voxel.

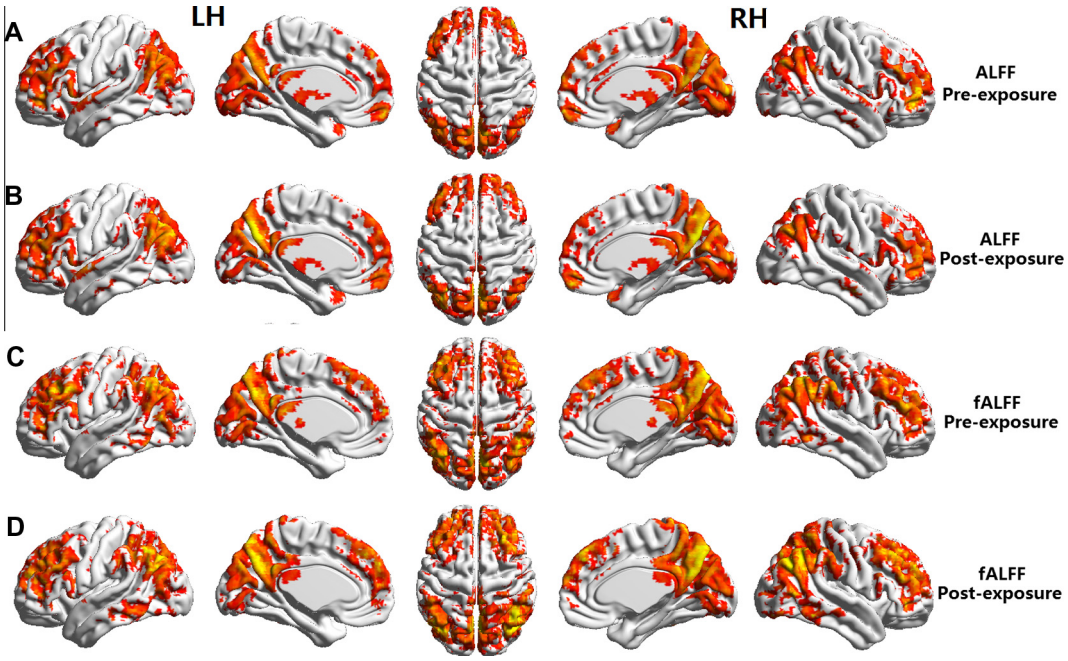

Fig. 3. Within-condition results during real exposure detected by one-sample *t* test for ALFF (A and B) and fALFF (C and D) method with AlphaSim corrected at $P < 0.05$. The conditions included pre-exposure (A and C) and post-exposure (B and D). The *t* value maps were colored according to the bar at the bottom. From these maps, we could clearly observe the areas having the significant higher standardized ALFF/fALFF value than the globe mean ALFF/fALFF value. LH = left hemisphere and RH = right hemisphere.

between-condition changes of spontaneous fluctuations induced by RF-EMF exposure successfully (Fig. 4 and Table 1 for the results of ALFF maps, while Fig. 5 and Table 1 for the results of fALFF maps). Fig. 4A showed the results which we did not perform the multiple corrections for ALFF maps. We observed that the decreased ALFF values in some regions (e.g. around the temporal cortex) and the increased values in some other regions (e.g. around the prefrontal cortex and occipito-parietal cortex). The results after multiple corrections were shown in Figs. 4B and 5, while positive values represent the ALFF/fALFF in pre-exposure is larger than that in post-exposure. After RF-EMF exposure, three brain regions showed significantly decreased ALFF values ($P < 0.05$, AlphaSim corrected), including cluster 1 which located in the junction of left superior temporal gyrus (STG_L) and left middle temporal gyrus (MTG_L), cluster 2 which located in the posterior part of right superior temporal gyrus (STG_R) and cluster 3 which located in the junction of right medial frontal gyrus (MFG_R) and the right paracentral lobule (PCL_R). And only one cluster nearby MFG_R and PCL_R was identified to have the significant decreased fALFF values. From the AlphaSim corrected results, we did not find any region that showed the significant increased values of ALFF or fALFF across the whole brain in post-exposure condition.

Additionally, we calculated the correlation coefficients among the three observed clusters from ALFF maps. Fig. 6A illustrated their mean and variance values in four different exposure conditions. Although we did not detect any significant between-condition differences of functional connectivity, there was a trend toward higher correlation between cluster 1 and cluster 2 after exposure in real session ($P = 0.059$). The mean values of functional connectivity in the real post-exposure were visualized on the

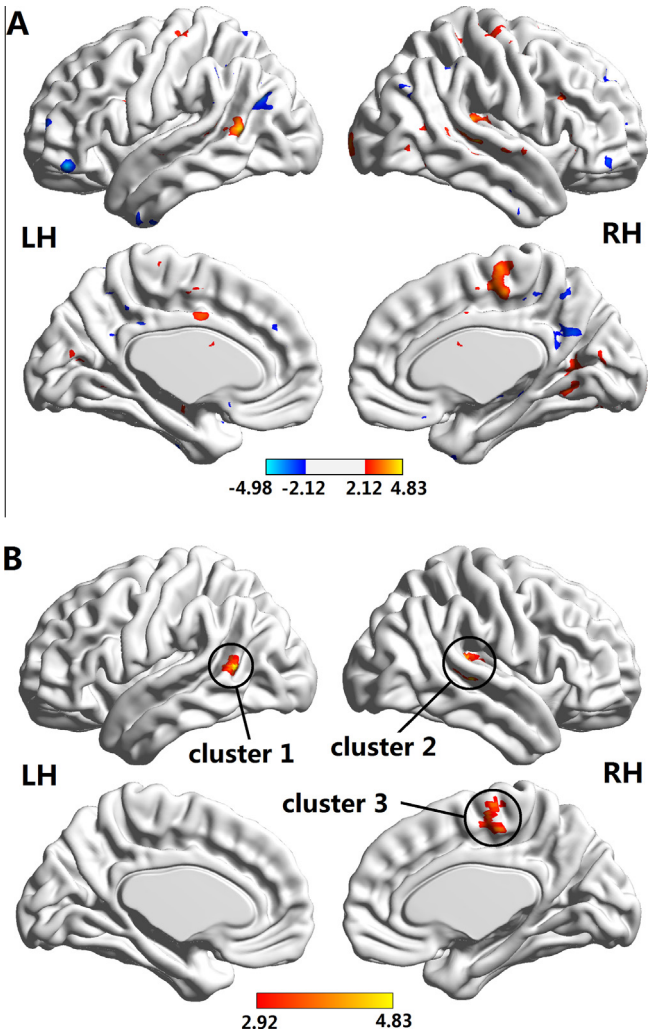

Fig. 4. ALFF between-condition differences between pre- and post-exposure during real exposure. (A) The result before multiple comparisons, and (B) The result after multiple comparisons ($P < 0.05$, AlphaSim corrected). The maps are colored according to the bars at the bottom. LH = left hemisphere and RH = right hemisphere. More details of these regions were described in Table 1.

ICBM-152 brain template from the top side of axial view (Fig. 6B) and the back side of coronal view (Fig. 6C).

4. Discussion

4.1. Experimental setup and SAR measurement

In our study, exposure experiment and MRI scan were performed by independent person, while subjects and data analyst were blind to the sequence of real and sham exposure. The double-blind, crossover, randomized and counterbalanced design is to avoid the subjective bias or other influences (e.g. the time elapse during the RF-EMF exposure). The choice of exposure site was inconsistent in previous studies: some selected the left side of brain (Curcio et al., 2005; Aalto et al., 2006) while others selected the right side (Volkow et al., 2011; Curcio et al., 2012). We selected the right side of the head as the place to put the dipole antenna since most right handed people tend to use the cell phone in their right ear (Siegel et al., 2012).

During the exposure, the LTE signal was emitted by a standard dipole instead of mobile phone to maintain the consistent exposure condition as much as possible. While the presence of the human body might influence the power reflection for the nearby dipole, adjusting the subject-specific delivered power is a key part to effectively compensate the reflective power. We found that the mean reflective power due to the human body is 3.3 dB with a standard deviation of 1.4 dB. The result indicated that if the reflective power was not considered in the study, the realistic emission power may diminish to less than 50% of the desired value. The high standard deviation suggested the anatomical difference was also an important consideration. For example, in the extreme case, one subject induced a reflective power up to 5.3 dB, which indicates that the actual emission was only 30% of the desired value. If the subjects cannot be assured the identical radiation, dose-effect relationship would be blurred. It is a possible reason that many experiments yield non-consistent and irreplaceable results (Valentini et al., 2007; Kwon and Hamalainen, 2011). Therefore, we applied the protocol dedicating to system check for SAR measurement in Standard 1528. IEEE recommended practice for determining the peak spatial-average specific absorption rate (SAR) in the human head from wireless communications devices: measurement techniques. NJ (1528) and adjusted the signal generator to obtain a desired output (Fig. 1). Our previous studies have established the Chinese anatomical model to evaluate the wideband RF-EMF exposure (Wu et al., 2011; Wu et al., 2012; Wu et al., 2013a; Wu et al., 2013b). Here, we established the anatomical head model from structural MR images and examined if the SAR power distribution is under the safety limits (Fig. 2).

4.2. Within-condition pattern of spontaneous fluctuations

Traditional fMRI studies have focused on the task-evoked responses in BOLD signal. However, the spontaneous modulation of BOLD signal was also observed in the brain even without any external stimulus or task (Fox and Raichle, 2007). The neural activity manifested as slow spontaneous fluctuations (typically <0.1 Hz) have provided some insight into the intrinsic functional organization in normal brain (Biswal et al., 1995; Hampson et al., 2002; Greicius et al., 2003; Zuo et al., 2010) and the possible alteration that was linked with the neurological and psychiatric diseases (He et al., 2007; Zang et al., 2007; Hoptman et al., 2010). Over the past decade, lots of processing methodologies have been proposed to deal with the resting-state fMRI data, and different methods may reflect different aspects of spontaneous brain activity (See article Margulies et al., 2010 for a review). While most methods focused on the resting-state functional connectivity (Biswal et al., 1995; Hampson et al., 2002; Greicius et al., 2003), ALFF method (Zang et al., 2007) and its improved version called fALFF (Zou et al., 2008) method were used to characterize the local spontaneous brain activity. In our study, within-condition analysis showed the significant higher standardized ALFF/fALFF values than the globe mean ALFF value in the posterior cingulate cortex/precuneus, medial prefrontal cortex, inferior parietal lobule and occipital areas (Fig. 3), which was consistent with the previous findings (Zang et al., 2007; Zou et al., 2008; Zuo et al., 2010). And we found most of them are the components of the default mode network (Greicius et al., 2003). The default mode network has been characterized by greater metabolic and neural activity during rest than active task performance, and considered as a physiological baseline for brain (Raichle et al., 2001; Greicius et al., 2003). Our results indicated these brain regions might maintain the higher spontaneous low frequency fluctuations during resting state than other areas.

ALFF indicates the absolute strength of spontaneous fluctuations within the frequency range between 0.01 and 0.1 Hz, and fALFF is a ratio which represents the relative contribution of specific spontaneous fluctuations to the whole frequency detectable frequency range. Some studies have reported that ALFF analysis might be susceptible to the physiological noise, and fALFF method could

Table 1
Brain regions showing significant between-condition difference in ALFF/fALFF values between pre- and post-exposure condition during real exposure.

	Cluster	Brain region	BA	MNI coordinate			Peak *t*-value	Cluster size (mm^3)
				X	*Y*	*Z*		
ALFF	1	STG_L, MTG_L	22, 39	−57	−57	9	4.83	783
	2	STG_R	21, 22, 41	57	−30	3	4.82	1242
	3	MFG_R, PCL_R	6	0	−24	51	3.95	1161
fALFF	4	MFG_R,PCL_R	6	3	−24	57	5.19	540

BA = Brodmann area; MNI = Montreal Neurological Institute; STG_L = left superior temporal gyrus; MTG_L = left middle temporal gyrus; STG_R = right superior temporal gyrus; MFG_R = right medial frontal gyrus; PCL_R = right paracentral lobule.

reduce this influence especially in the vicinity of blood vessels and cerebral ventricles (Zou et al., 2008; Zuo et al., 2010). Our results illustrated there were significant higher ALFF values surrounding the bilateral lateral fissure while they were disappeared on fALFF maps (Fig. 3). This phenomenon could be explained by the fact that the middle cerebral artery pass laterally through the lateral fissure (Nowinski et al., 2011).

4.3. Brain regions of between-condition difference induced by exposure

The paired *t* tests have successfully detected the between-condition difference caused by RF-EMF exposure on both ALFF and fALFF maps during the real exposure (Fig. 4, Fig. 5, and Table 1). Although the increased ALFF values were present in the prefrontal cortex and occipito-parietal cortex both laterally and medially (Fig. 4A), they did not reach significance after multiple comparisons, possibly because of the small sample size. After AlphaSim corrected, there were decreased ALFF values surrounding STG_L, MTG_L, STG_R, MFG_R and PCL_R (Fig. 4B and Table 1), and decreased fALFF values around MFG_R and PCL_R (Fig. 5 and Table 1). The results indicated that RF-EMF exposure modulated the spontaneous brain activity in these brain regions.

Before explaining the findings in the present study with respect to other previous neurophysiological studies, we need to point out several discrepancies among them which might lead to the inconsistent results. Firstly, we evaluated the induced effects of LTE-related RF-EMF exposure at 2.573 GHz band, whereas most previous studies investigated the effects of GSM signal at 900/1800 MHz band (Croft et al., 2002; Huber et al., 2002; Haarala et al., 2003; Curcio et al., 2005; Aalto et al., 2006; Kleinlogel et al., 2008; Volkow et al., 2011; Curcio et al., 2012) or UMTS signal at 2100 MHz band (Kleinlogel et al., 2008). Secondly, during the mobile phone use, skin temperature can increase around the exposure site. Only a small part of the temperature rise is contributed by the RF-EMF exposure while most is mainly due to the heat conduction from operating phone (Anderson and Rowley, 2007). Therefore, it is hard to determine whether the observed effects are caused by heating-induction or RF-EMF exposure when using mobile phone as exposure source. In our study, we used the dipole antenna instead of mobile phone. The dipole antenna does not lead to the temperature rise and thus is completely free from heating-induction. Thirdly, the dipole antenna was put at a distance of 1 cm to the subject's ear, yet when using a real mobile phone the antenna is not located in front of the ear, instead, backwards in close proximity to the temporal-occipital cortex (Haarala et al., 2003; Aalto et al., 2006). Such discrepancy of exposure site might explain the differences of brain regions found in the present study with respect to other studies. Finally, we selected the resting state fMRI to investigate the possible effects of RF-EMF exposure, while previous studies often used EEG (Croft et al., 2002; Huber et al., 2002; Curcio et al., 2005; Kleinlogel et al., 2008) or PET (Huber et al., 2002; Haarala et al., 2003; Aalto et al., 2006; Volkow et al., 2011). Different neurophysiological techniques characterize different properties of brain activity, thus we cannot compare with their findings directly, and need to investigate whether the observed effects of RF-EMF exposure are comparable among different studies.

Although fMRI technique has been a powerful tool to investigate the brain function in neuroscience during the past 20 years (Bandettini, 2012), till now, only one study attempted to examine the RF-EMF exposure effects on brain activity by using BOLD fMRI signal (Curcio et al., 2012). They designed an event-related fMRI experiment with G0-NoGo task, and measured the BOLD response while performing the cognitive task before and after the exposure. The results revealed no significant change in BOLD response induced by mobile phone exposure. Our study has found the alteration of spontaneous low frequency fluctuations caused by acute RF-EMF exposure. It was not very strange that we did not obtain consistent results with Curcio's study (Curcio et al., 2012). The first reason is that their exposure source was a typical basic GSM signal with a carrier frequency of 902.40 MHz (Curcio et al., 2012), while we used the standard dipole antenna to emit a LTE signal at 2.573 GHz. The conditions of RF-EMF exposure are different between the two studies. Second and more importantly, Curcio et al. Curcio et al. (2012) examined the task-evoked responses in BOLD fMRI signal, whereas our study focused on the spontaneous low frequency fluctuations in brain during resting state. Previous study suggested that a direct comparison should be performed with caution between the results obtained from the resting-state study and the task-state study (Zang et al., 2007). Generally, the task-evoked responses are the signal changes from resting-state to task-state. The signals during resting-state are usually viewed as the baseline and not taken into account in task-response study. More and more studies have revealed that they are more related to spontaneous neural activity and provide us with important insight into the intrinsic functional architecture of the brain (Fox and Raichle, 2007; Zuo et al., 2010). Therefore, our study and Curcio's study investigated difference states for brain activity and their possible changes induced by RF-EMF exposure.

Neural activity in the brain is often accompanied by the changes in glucose utilization, blood oxygenation utilization and cerebral blood flow (CBF) Bélanger et al., 2011; Murphy et al., 2013. In general, the increased neural activity is associated with the increased cerebral metabolic activity (including glucose consumption and oxygen consumption), and also gives rise to the increase of CBF with the mechanism of neurovascular coupling (Bélanger et al., 2011; Murphy et al., 2013). PET imaging allows us to measure the changes of CBF or brain glucose metabolism (Bélanger et al., 2011). BOLD signals measured with fMRI depend on many interacting factors, which are sensitive not only to the changes of CBF but also to the oxygen consumption (Murphy et al., 2013). Therefore, there is a complex nonlinear coupling relationship between CBF and BOLD signals (Mechelli et al., 2001). When CBF is larger than the increasement of oxygen consumption, oxyhaemoglobin is oversupplied to the regional area leading to a reduction in deoxyhaemoglobin concentration, thus resulting in the increased BOLD signals (Murphy et al., 2013). Previous studies with PET

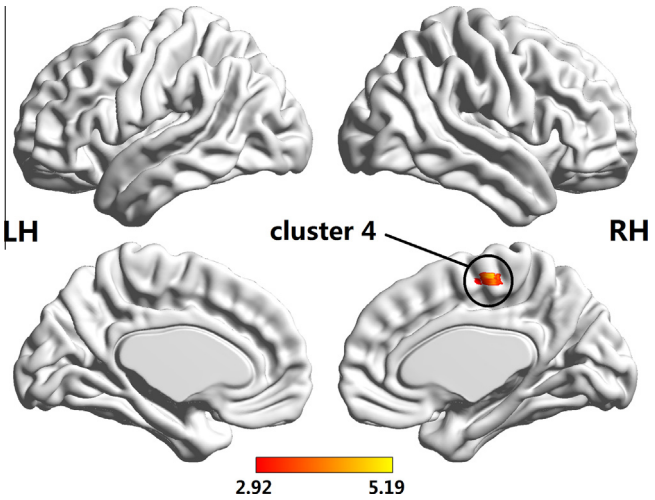

Fig. 5. fALFF between-condition differences between pre- and post-exposure during real exposure ($P < 0.05$, AlphaSim corrected). The maps are colored according to the bar at the bottom. LH = left hemisphere and RH = right hemisphere. More details of this region were described in Table 1.

techniques have investigated the effects of RF-EMF exposure on brain rCBF (Huber et al., 2002; Haarala et al., 2003; Aalto et al., 2006). In our study, we found the decreased low frequency oscillations in STG_R, STG_L and MTG_L with ALFF analysis. They localized in the lateral temporal cortex and their posterior parts encompassed the auditory cortex which played an important role in auditory processing. One previous PET study has reported that the exposure to an active mobile phone produced a relative decreased rCBF bilaterally in the auditory cortex (Haarala et al., 2003). They explained that the decreased rCBF might be due to a weak sound signal from an active phone (noise caused by the battery). A subsequent study eliminated this confounding factor and found a decreased rCBF in the ipsilateral inferior temporal cortex and an increased rCBF in the bilateral prefrontal cortex (Aalto et al., 2006). In our experiment, we used the dipole antenna as the exposure source. Therefore, there was no probable confounding effect of auditory noise, and our result was to some extent consistent with the result reported by some previous studies (Haarala et al., 2003; Aalto et al., 2006). This revealed that the acute RF-EMF exposure might modulate the neural activity which corresponded to the auditory processing, not only reflecting on the changes of rCBF but also on the BOLD signals. When using fALFF analysis, the changes of spontaneous fluctuations induced by RF-EMF exposure disappeared in STG_R, STG_L and MTG_L, indicating

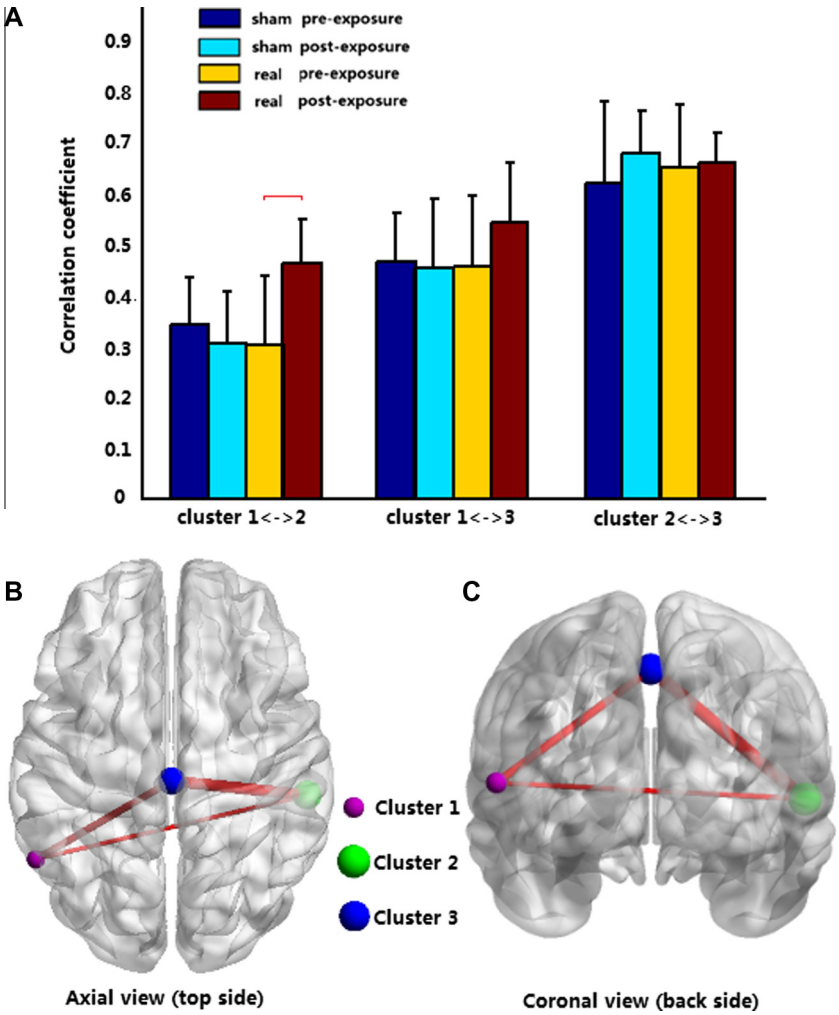

Fig. 6. (A) The mean and variance values of correlation coefficients among three clusters. Different color bars show different exposure conditions. The mean values of correlation coefficients in real post-exposure were plotted on brain surface (ICBM-152 brain template) from the top side of axial view (B) and the back side of coronal view (C). The nodes are scaled by cluster size and the lines are scaled by correlation coefficient.

that the exposure effect was likely to relative slight in these areas. Both ALFF and fALFF analysis have found the decreased spontaneous low frequency fluctuations in MFG_R and PCL_R. Previous fMRI studies have reported MFG was considered for information processing in decision-making (Talati and Hirsch, 2005), and PCL was involved in the lower extremity movements (Lim et al., 1994) and was one of the secondary somatosensory areas (Damasio, 1999). The result on MFG_R and PCL_R illustrated the RF-EMF exposure might modulate the neural activity which corresponded to the decision-making and somatosensory processing. Several studies have found that the increased rCBF in the prefrontal cortex (Huber et al., 2002; Aalto et al., 2006) and also the higher brain glucose metabolism in the orbitofrontal cortex and temporal pole (Volkow et al., 2011). In our study, no significant increased ALFF/fALFF values were found across the whole brain. Previous studies have revealed that both oxidative and nonoxidative glucose metabolism processes are involved during neural activity (Bélanger et al., 2011; Figley and Stroman, 2011). Therefore, the changes of glucose metabolism induced by RF-EMF exposure might not always be associated with the alternation of BOLD signals, and the underlying mechanism still need to be investigated in the future.

There had been lots of EEG studies to investigate the effect of RF-EMF exposure (Valentini et al., 2007; Kwon and Hamalainen, 2011). The consistent results were mainly obtained from the resting and sleeping EEG (Croft et al., 2002; Huber et al., 2002; Curcio et al., 2005), while not from event-related or evoked potentials studies (Valentini et al., 2007; Kleinlogel et al., 2008; Kwon and Hamalainen, 2011). Considering the complexity of human brain, it is better to make clear the RF-EMF effect on spontaneous brain activity before trying to explore the possible effect induced by RF-EMF during cognitive processing. Croft et al. (2002) found the mobile phone exposure altered the resting EEG with decreasing activity in delta band (1–4 Hz) and increasing activity in theta/alpha band (8–12 Hz). Recent studies indicated the resting-state fMRI signal correlated with the power coherence in low-frequency bands, particularly the delta band (Lu et al., 2007). And in bilateral prefrontal and parietal cortex, there were widespread negative correlations between BOLD fMRI signal and EEG power of alpha band (Laufs et al., 2003). The decreasing EEG activity in delta band (Croft et al., 2002) and increasing EEG activity in alpha band (Croft et al., 2002; Curcio et al., 2005) could be used to explain plausibly our findings of the decreased ALFF/fALFF induced by RF-EMF exposure.

During the exposure, the radiation source was on the right side of head with a distance of 1 cm to the ear. Cluster 2 (STG_R) was close to this exposure site, while cluster 1 (STG_L, MTG_L) was approximate on the homologous areas in the opposite hemisphere and cluster 3 (MFG_R, PCL_R) was on the ipsilateral side but relative far away from the exposure site. The results demonstrated the RF-EMF exposure modulated the brain neural activity not only in the closer brain region but also in the remote region and even in the contralateral brain region. The remote effects of RF-EMF have been observed in many previous studies (Croft et al., 2002; Huber et al., 2002; Haarala et al., 2003; Aalto et al., 2006), although the reported brain regions were not completely consistent. Previous studies have found GSM RF-EMF exposure modulates the interhemispheric functional coupling of EEG alpha rhythms (Vecchio et al., 2007). In our study, we investigated the correlation among the three observed clusters. Although we did not detect any significant differences, there was a trend toward higher correlation between cluster 1 and cluster 2 after exposure in real session (Fig. 6). The results showed that RF-EMF exposure might not only affect the regional neural activity but also slightly alter the functional connectivity between different brain regions. It provides us with some evidences to explain the underlying neural mechanism for the remote effects of RF-EMF exposure.

4.4. Limitations and future work

Given the relevance of the present study for both the scientific and industrial fields, and considered that this is the first study finding the acute effect of RF-EMF exposure on BOLD response, some limitations require attention and need to be improved in the future. These issues can be summarized in two categories, experimental design and data analysis. For experimental design, we used the dipole antenna to generate the LTE signals at 2.573 GHz band and put it near the right ear. Our findings cannot be directly used to infer whether the similar effects would be observed by other frequency RF-EMF (e.g., 900, 1800 MHz) or other exposure site (e.g., close to the temporal-occipital cortex), thus more experiments need to be performed to investigate them. In addition, we applied the resting-state fMRI while subjects were instructed to stay awake and keep relax. Although all subjects reported they did not fall asleep, it is difficult to completely rule out the possibility that subjects fell asleep or experienced sleepiness during MRI scan. Further studies can collect EEG data simultaneously to monitor the level of consciousness during the resting-state fMRI (Horovitz et al., 2008). For data analysis, we used FDTD method to examine whether SAR power distribution induced by RF-EMF exposure was under the safety limit, and performed the ROI-based functional connectivity analysis among the observed brain regions in order to investigate the remote effects of RF-EMF exposure. Further works include investigating the correlation between spontaneous low frequency fluctuations and the SAR power distribution in all subjects to establish the dose-effect relationship, and examining the possible RF-EMF effect on large-scale functional connectivity across the whole brain.

In conclusion, we designed a controlled LTE RF-EMF radiation source and applied the resting state fMRI technique to examine the spontaneous low frequency fluctuations changes in normal human brain induced by LTE RF-EMF exposure. The ALFF and fALFF approaches have been selected to localize the alteration of spontaneous low frequency fluctuations between pre- and post-exposure condition. The experimental results provide the evidences that acute exposure induced by LTE RE-EMF affects the brain activity during resting state. However, whether the induced alteration on spontaneous low frequency fluctuations is directly harmful to brain function still needs to be investigated.

Acknowledgements

We would like to thank all the participants enrolled in this study. This study was supported by National Natural Science Foundation of China (Grant No. 61201066, 61001159, and 81171319), China Postdoctoral Science Foundation (Grant No. 2012M510381), and National Key Basic Research Project (Grant No. 2011CB503705). The authors declare no conflict of interest.

References

Aalto S, Haarala C, Brück A, Sipilä H, Hämäläinen H, Rinne JO. Mobile phone affects cerebral blood flow in humans. J Cereb Blood Flow Metab 2006;26:885–90.
Anderson V, Rowley J. Measurements of skin surface temperature during mobile phone use. Bioelectromagnetics 2007;28:159–62.
Ashburner J, Friston KJ. Unified segmentation. Neuroimage 2005;26:839–51.
Bandettini PA. Twenty years of functional MRI: the science and the stories. Neuroimage 2012;15:575–88.
Barnes FS, Gandhi OP, Hietanen M, Kheifets L, Matthes R, McCormick DL, et al. Identification of research needs relating to potential biological or adverse health effects of wireless communications devices. Washington DC: National Academies Press; 2008.
Bélanger M, Allaman I, Magistretti PJ. Brain energy metabolism: focus on astrocyte-neuron metabolic cooperation. Cell Metab 2011;14:724–38.
Biswal BB, Yetkin FZ, Haughton VM, Hyde JS. Functional connectivity in the motor cortex of resting human brain using echo-planar MRI. Magn Reson Med 1995;34:537–41.

Croft RJ, Chandler JS, Burgess AP, Barry RJ, Williams JD, Clarke AR. Acute mobile phone operation affects neural function in humans. Clin Neurophysiol 2002;113:1623–32.
Curcio G, Ferrara M, Moroni F, D'Inzeo G, Bertini M, De Gennaro L. Is the brain influenced by a phone call? An EEG study of resting wakefulness. Neurosci Res 2005;53:265–70.
Curcio G, Nardo D, Perrucci MG, Pasqualetti P, Chen TL, Gratta CD, et al. Effects of mobile phone signals over BOLD response while performing a cognitive task. Clin Neurophysiol 2012;123:129–36.
Damasio A. The feeling of what happens: body and emotion in the making of consciousness. New York NY: Harcourt Brace; 1999.
Figley CR, Stroman PW. The role(s) of astrocytes and astrocyte activity in neurometabolism, neurovascular coupling, and the production of functional neuroimaging signals. Eur J Neurosci 2011;33:577–88.
Fox MD, Raichle ME. Spontaneous fluctuations in brain activity observed with functional magnetic resonance imaging. Nat Rev Neurosci 2007;8:700–11.
Greicius MD, Krasnow B, Reiss AL, Menon V. Functional connectivity in the resting brain: a network analysis of the default mode hypothesis. Proc Natl Acad Sci USA 2003;100:253–8.
Haarala C, Aalto S, Hautzel H, Julkunen L, Rinne JO, Lain M, et al. Effects of a 902 MHz mobile phone on cerebral blood flow in humans – a PET study. NeuroReport 2003;14:2019–23.
Hampson M, Peterson BS, Skudlarski P, Gatenby JC, Gore JC. Detection of functional connectivity using temporal correlations in MR images. Hum Brain Mapp 2002;15:247–62.
He Y, Wang L, Zang YF, Tian LX, Zhang XQ, Li KC, et al. Regional coherence changes in the early stages of Alzheimer's disease: a combined structural and resting-state functional MRI study. Neuroimage 2007;35:488–500.
Hoptman MJ, Zuo XN, Butler PD, Javitt DC, D'Angelo D, Mauro CJ, et al. Amplitude of low-frequency oscillations in schizophrenia: a resting state fMRI study. Schizophr Res 2010;117:13–20.
Horovitz SG, Fukunaga M, de Zwart JA, van Gelderen P, Fulton SC, Balkin TJ, et al. Low frequency BOLD fluctuations during resting wakefulness and light sleep: a simultaneous EEG-fMRI study. Hum Brain Mapp 2008;29:671–82.
Huber R, Treyer V, Borbély AA, Schuderer J, Gottselig JM, Landolt HP, et al. Electromagnetic fields, such as those from mobile phones, alter regional cerebral blood flow and sleep and waking EEG. J Sleep Res 2002;11:289–95.
ICNIRP (International Commission on Non-Ionizing Radiation Protection). Guidelines for limiting exposure to time-varying electric, magnetic, and electromagnetic fields (up to 300 GHz). Health Phys 1998;74:494–522.
IEEE Standard 1528. IEEE recommended practice for determining the peak spatial-average specific absorption rate (SAR) in the human head from wireless communications devices: measurement techniques. NJ, USA: Piscataway; 2003.
Kainz W, Christ A, Kellom T, Seidman S, Nikoloski N, Beard B, et al. Dosimetric comparison of the specific anthropomorphic mannequin (SAM) to 14 anatomical head models using a novel definition for the mobile phone positioning. Phys Med Biol 2005;50:3423–45.
Kleinlogel H, Dierks Th, Koenig Th, Lehmann H, Minder A, Berz R. Effects of weak mobile phone – electromagnetic fields (GSM, UMTS) on event related potentials and cognitive functions. Bioelectromagnetics 2008;29:488–97.
Kwon MS, Hamalainen H. Effects of mobile phone electromagnetic fields: critical evaluation of behavioral and neurophysiological studies. Bioelectromagnetics 2011;32:253–72.
Laufs H, Krakow K, Sterzer P, Eger E, Beyerle A, Salek-Haddadi A, et al. Electroencephalographic signatures of attentional and cognitive default modes in spontaneous brain activity fluctuations at rest. Proc Natl Acad Sci USA 2003;100:11053–8.
Ledberg A, Akerman S, Roland PE. Estimation of the probabilities of 3D clusters in functional brain images. Neuroimage 1998;8:113–28.
Lim SH, Dinner DS, Pillay PK, Lüders H, Morris HH, Klem G, et al. Functional anatomy of the human supplementary sensorimotor area: results of extraoperative electrical stimulation. Electroencephalogr Clin Neurophysiol 1994;91:179–93.
Logothetis NK, Wandell BA. Interpreting the BOLD signal. Annu Rev Physiol 2004;66:735–69.
Lu HB, Zuo YT, Gu H, Waltz JA, Zhan W, Scholl CA, et al. Synchronized delta oscillations correlate with the resting-state functional MRI signal. Proc Natl Acad Sci USA 2007;104:18265–9.
Mao Y, Bian Q, Wang ZQ. A FDTD system-SEMF. No. 0287104, Registration of software copyright, China, 2011.
Margulies DS, Bottger J, Long XY, Lv YT, Kelly C, Schafer A, et al. Resting developments: a review of fMRI post-processing methodologies for spontaneous brain activity. Magn Reson Mater Phys 2010;23:289–307.
Mechelli A, Price CJ, Friston KJ. Nonlinear coupling between evoked rCBF and BOLD signals: a simulation study of hemodynamic responses. Neuroimage 2001;14:862–72.
Murphy K, Birn RM, Bandettini PA. Resting-state fMRI confounds and cleanup. Neuroimage 2013;80:349–59.
Nowinski WL, Chua BC, Marchenko Y, Puspitsari F, Volkau I, Knopp MV. Three-dimensional reference and stereotactic atlas of human cerebrovasculature from 7 Tesla. Neuroimage 2011;55:986–98.
Parkvall S, Furuskа RA, Dahlman E. Evolution of LTE toward IMT-advanced. IEEE Comm Mag 2011;49:84–91.
Patrick K, Griswold WG, Raab F, Intille SS. Health and the mobile phone. Am J Prev Med 2008;35:177–81.
Raichle ME, MacLeod AM, Snyder AZ, Powers WJ, Gusnard DA, Shulman GL. A default mode of brain function. Proc Natl Acad Sci USA 2001;98:676–82.
Siegel B, Shah P, Bowyer S, Seidman M. Hemispheric dominance and cell phone use. ARO Abstracts 2012;35:112–3.
Taflove A, Hagness SC. Computational electrodynamics: the finite-difference time-domain method. 3rd ed. Norwood MA: Artech House; 2005.
Talati A, Hirsch J. Functional specialization within the medial frontal gyrus for perceptual go/no-go decisions based on "what", "when", and "where" related information: an fMRI study. J Cogn Neurosci 2005;17:981–93.
Valentini E, Curcio G, Moroni F, Ferrara M, De Gennaro L, Bertini M. Neurophysiological effects of mobile electromagnetic fields on humans: a comprehensive review. Bioelectromagnetics 2007;28:415–32.
Van Dijk KR, Hedden T, Venkataraman A, Evans K, Lazar S, Buckner R. Intrinsic functional connectivity as a tool for human connectomics: theory, properties, and optimization. J Neurophysiol 2010;103:297–321.
Vecchio F, Babiloni C, Ferreri F, Curcio G, Fini R, Del Percio C, et al. Mobile phone emission modulates interhemispheric functional coupling of EEG alpha rhythms. Eur J Neurosci 2007;25:1908–13.
Volkow ND, Tomasi D, Wang GJ, Vaska P, Fowler JS, Telang F, et al. Effects of cell phone radiofrequency signal exposure on brain glucose metabolism. JAMA 2011;305:808–13.
Wu TN, Tan LW, Shao Q, Zhang C, Zhao C, Li Y, et al. Chinese adult anatomical models and the application in evaluation of wideband RF EMF exposure. Phys Med Biol 2011;56:2075–89.
Wu TN, Lv B, Chen ZY. Dosimetric studies involving in the experiments for the evaluation of the brain activation by LTE exposure. In: Proceedings of international symposium on electromagnetic compatibility (EMC EUROPE), Rome, Italy: IEEE; 2012.
Wu TN, Shao Q, Yang L. Simplied segmented human models for whole body and localized SAR evaluation of 20 MHz–6 GHz electromagnetic field exposures. Radiat Prot Dosimetry 2012;153:266–72.
Wu TN, Tan LW, Shao Q, Li Y, Yang L, Zhao C, et al. Slice-based supine to standing postured deformation for Chinese anatomical models and the dosimetric results by wide band frequency electromagnetic field exposure: morphing. Radiat Prot Dosimetry 2013a;154:26–30.
Wu TN, Tan LW, Shao Q, Li Y, Yang L, Zhao C, et al. Slice-based supine to standing postured deformation for Chinese anatomical models and the dosimetric results by wide band frequency electromagnetic field exposure: simulation. Radiat Prot Dosimetry 2013b;154:31–6.
Yan CG, Zang YF. DPARSF: a MATLAB toolbox for "pipeline" data analysis of resting-state fMRI. Front Syst Neurosci 2010;4:13.
Zang YF, He Y, Zhu CZ, Cao QJ, Sui MQ, Liang M, et al. Altered baseline brain activity in children with ADHD revealed by resting-state functional MRI. Brain Dev 2007;29:83–91.
Zou QH, Zhu CZ, Yang YH, Zuo XN, Long XY, Cao QJ, et al. An improved approach to detection of amplitude of low-frequency fluctuation (ALFF) for resting-state fMRI: fractional ALFF. J Neurosci Meth 2008;172:137–41.
Zuo XN, Martino AD, Kelly C, Shehzad ZE, Gee DG, Klein DF, et al. The oscillating brain: complex and reliable. Neuroimage 2010;49:1432–45.
Zuo XN, Xu T, Jiang LL, Yang Z, Cao XY, He Y, et al. Toward reliable characterization of functional homogeneity in the human brain: preprocessing, scan duration, imaging resolution and computational space. Neuroimage 2013;65:374–86.